Advanced Metaloxide Nanomaterials for Gas Sensors with Controlled Properties

Dzmitry Kotsikau and Maria Ivanovskaya

Research Institute for Physical-Chemical Problems, Belarusian State University,
14 Leningradskaya, 220030 Minsk, Belarus

1. INTRODUCTION

As it was shown earlier, the modification of the sol-gel technology based on inorganic precursors is a promising approach to obtain advanced metaloxide materials for gas sensors[1,2]. This variation of the sol-gel technology allows the preparation of nanomaterials in forms of sol, powder, film and ceramics. It is based on the precipitation of metal hydroxides and consecutive transformation of the precipitate into sol, gel, xerogel and crystalline oxide[3].

The sol-gel derived metaloxide materials are typically characterized by the following structural peculiarities[2,4]:

- Nanosized dimension and nanostructuredness, highly developed surface.
- High concentration of structural point defects: oxygen vacancies(V_O); electrons, stabilized in oxygen vacancies(V_O^- or *F*-center); metal cations in lower than the main oxidation state ($M^{(n-1)+}$).
- Reversibility of $[M^{(n1)+}–V_O]\leftrightarrow[M^{n+}–V_O]$ transition in cycling red/ox gas ambient that provides preserving high activity of the samples during long-term operations.
- Formation and stabilization of metastable phases, which are active in catalysis and adsorption due to high dispersity, poor crystallinity and loose structure.
- High thermal stability of structure due to charge transfer between the components.
- Stabilization of noble metal particles(Pd, Pt, Au, Ru etc.) in nanosized and partially oxidized state within oxide matrixes.

The mentioned structural peculiarities cause unique functional features of the sol-gel derived materials, in particular, their advanced gas-sensing properties. The sol-gel approach also provides wide possibilities to modify the nanostructure and phase composition of metaloxide materials, and, consequently, to control their gas-sensing behavior. This is caused by the formation of the oxide structure at the stages of a sol and xerogel preparation at low temperatures[4].

In this paper, the possibilities to control the sensitivity and selectivity of In_2O_3–Fe_2O_3 based nanocomposites by varying their microstructure, phase composition, grain size and surface state were considered. This was achieved by theoretically grounded selection of both chemical composition and conditions of synthesis of the materials. Their catalytic and adsorption properties are also considered.

The choice of In_2O_3 and Fe_2O_3 oxides is caused by their structural and electrophysical features, which allow to expect promising gas-sensing behavior of the In_2O_3–Fe_2O_3 composites. Iron oxide can be prepared in a number of structural modifications with different catalytic, adsorption and electrophysical properties[5-7]. Along with main α-Fe_2O_3 phase, thermodynamically metastable iron oxide modifications like cubic *C*-γ-Fe_2O_3, tetragonal *Q*-γ-Fe_2O_3 and Fe_3O_4 can be kinetically stable under typical working temperatures of semiconducting sensors. Metastable hexagonal indium oxide(*H*-In_2O_3) can be obtained in the presence of Fe_2O_3 along with thermodynamically stable cubic phase(*C*-In_2O_3)[8].

In our previous work it was shown that oxide materials can be effective gas-sensing materials for thick-film and ceramic sensors[9,10]. The inorganic modification of the sol-gel process allowed us to develop single-electrode ceramic micro-sensors with hollow structure[11,12]. This type of sensors was found to be characterized by low power consumption and fast dynamics.

In this study the gas-sensing properties of the synthesized materials were estimated using thin-film sensors.

2. EXPERIMENTAL DETAILS

2.1 Composition of sensing layers

As it was shown earlier, the doping of In_2O_3 with Fe_2O_3 (Fe:In = 1:9 molar ratio) evokes decreasing the composite layer conductivity and sensitivity to most of gases[13]. Therefore, the compositions with greater content of iron (Fe:In = 1:1 and 9:1) were selected for this study. The formation of complex structures of the In_2O_3–Fe_2O_3 composites based on different Fe_2O_3 phase modifications as a function of the synthesis conditions were expected.

2.2 Synthesis of oxide composites

Two series of the In_2O_3–Fe_2O_3 composites were prepared. Series *I* was prepared by combined hydrolysis of iron and indium salts with a base agent(ammonia), and further transformation of the precipitates into sol state. Series *II* was prepared by separate hydrolysis of indium or iron salts, and stabilization of individual indium or iron hydroxides/oxides in sol state; then the individual sols were mixed together in the required proportions.

Hydrolysis of Fe^{3+} inorganic salts leads to the formation of amorphous iron hydroxide, which crystallizes into highly dispersed α-Fe_2O_3 phase under heating of the dried material at 300 ºC. Hydrolysis of Fe^{2+} inorganic salts results in $Fe(OH)_2$, which transforms into metastable γ-Fe_2O_3 with grain size of 4045 nm under oxidation of the suspension with air at 100 ºC and heating at 300 ºC. The formation of cubic γ-Fe_2O_3 also proceeds through Fe_3O_4 intermediate under combined hydrolysis of Fe^{3+} and Fe^{2+} salts with subsequent oxidation and thermal treatment. This way allows to generate smaller γ-Fe_2O_3 particles (~10 nm) with high content of OH-groups in the oxide structure.

Adsorption and catalytic properties of the nanosized γ-Fe_2O_3 samples obtained by our approach at low temperatures differ drastically from the high-temperature phases with highly ordered crystalline structure. Specific properties of the sol-gel derived In_2O_3–Fe_2O_3 composites are also caused by certain structural features, which are typical of iron oxide formed in the presence of indium hydroxide at low temperatures. Mutual influence of indium and iron on the hydrolysis, and on the structure of the product takes place in the process of combined precipitation of iron and indium hydroxides. There is literature reporting high mutual solubility of In_2O_3 and α-Fe_2O_3 phases[14] and lack of solubility of In_2O_3 in spinel-type γ-Fe_2O_3 structure[15].

The prepared colloidal solutions(sols) of the composites of both series were deposited onto sensor substrates to form thin-film sensors. The samples in powder form used for some structural studies were prepared by drying the corresponding sols.

2.3 Structural characterization

Phase composition of the samples was characterized by means of X-ray diffraction(XRD) analysis. Fine structural features of the Fe_2O_3–In_2O_3 composites, which are typically nanosized and poorly crystallized, were revealed by high-resolution transmission electron microscopy(TEM), electron diffraction(ED), Mössbauer spectroscopy, infrared spectroscopy(IR), and electron paramagnetic resonance (EPR). XRD analysis was carried out on a *HZG-4A* diffractometer by using CoK_α radiation. TEM/ED examinations were performed with a *LEO 906E* and a *JEOL 4000 EX* high-resolution transmission electron microscopes. The resonance spectra were recorded in air at 298 K and processed by using a commercial *SM 2201* Mössbauer spectrometer equipped with a 15 mCi ^{57}Co(Rh) source. EPR spectra were recorded on a *VARIAN E112* spectrometer with a frequency of 9.35 GHz at 77 K. IR characterization was carried out on an *AVATAR FTIR-330* spectrometer supplied with smart diffuse reflectance accessory.

2.4 Fabrication and testing of sensors

In order to obtain thin-film sensors, the sols were deposited by spin-coating onto polycrystalline Al_2O_3 substrates($3\times3\times0.25$ mm^3) supplied with Pt interdigitated electrode structure on front side and Pt-heater on rear side. The thickness of the thin films was estimated to be about 200 nm. The sensor elements were successively annealed at 300-400 ºC for 96 h in air. The gas-sensing responses of the films to C_2H_5OH, NO_2 and O_3 gases were studied and correlated with the structural properties of the active materials. Contact electric potential was applied to the interdigitated electrode structure and current through a sensing layer in air and in air-gas mixtures

was measured. The response(S) of the sensors was calculated as I_{air}/I_{gas} and I_{gas}/I_{air} when detecting oxidizing(NO_2, O_3) and reducing(C_2H_5OH) gases, respectively. The measurements were carried out in a flow chamber(0.2 l) at 0.3 $l \cdot min^{-1}$ flow rate, 20 °C temperature and 30 % relative humidity.

3. RESULTS AND DISCUSSIONS

3.1 Structural characterization of the composites

Phase composition and grain size of the studied Fe_2O_3–In_2O_3 samples as a function of the synthesis conditions are summarized in Table 1. There is a clear mutual influence of the components on the formation of the binary composite structure under thermal treatment of the sols and xerogels. Inhibition of crystallization processes of oxide phases is typical of the composites as compared to individual iron and indium oxides.

Table 1. Structural peculiarities of the $Fe_2O_3In_2O_3$ composites. Annealing temperature is 300 °C

No	Precursors	Fe:In mol.	Phases*	Grain size, nm
Series I(*combined hydrolysis*)				
1	Fe^{3+}, In^{3+}	9:1	α-Fe_2O_3	2-4
2		1:1	*C*-In_2O_3	5-8
3	Fe^{2+}, In^{3+}	9:1	α-Fe_2O_3	3-6
4		1:1	*C*-In_2O_3 α-Fe_2O_3	5-8 5-6
5	Fe^{2+}, Fe^{3+}, In^{3+}	9:1	*Q*-γ-Fe_2O_3 *C*-γ-Fe_2O_3 α-Fe_2O_3	10×30 2-4 2-4
6		1:1	*C*-In_2O_3 α-Fe_2O_3	5-8
Series II(*mixing separately prepared sols*)				
7	$In(OH)_3$, Fe_3O_4	9:1	*C*-γ-Fe_2O_3 *C*-In_2O_3	4-5 5-8
8		1:1	*C*-In_2O_3 *C*-γ-Fe_2O_3	7-8 5-6
9	$In(OH)_3$, $Fe(OH)_2$	9:1	*C*-γ-Fe_2O_3 *C*-In_2O_3	8-10 5-6
10		1:1	*C*-In_2O_3 *C*-γ-Fe_2O_3	7-8
11	$In(OH)_3$, $Fe(OH)_3$	9:1	α-Fe_2O_3	3-8
12		1:1	*C*-In_2O_3 α-Fe_2O_3	5-8 3-6

*Phases denoted here as α-Fe_2O_3 and *C*-In_2O_3 are actually substitutional solid solutions α-$Fe_{2x}In_xO_3$ and *C*-$In_{2x}Fe_xO_3$, respectively.

As it is seen from Table 1, hydrolysis of inorganic Fe^{3+} salts always results in α-Fe_2O_3 structure at 300 °C(samples 1, 11, 12). This phase is nanosized and X-ray amorphous. Within the Fe_2O_3–In_2O_3 composite, mutual doping of α-Fe_2O_3 and *C*-In_2O_3 takes place resulting in substitutional solid solutions in a wide range of concentrations[14].

At Fe:In = 1:1 molar ratio the main phase occurred in the $Fe_2O_3In_2O_3$ composites is cubic indium oxide(*C*-In_2O_3) with the unit cell parameter a decreased comparing to the reference data(samples 2, 4, 6, 8, 10, 12). The formation of hexagonal indium oxide(*H*-In_2O_3) was not revealed.

Combined hydrolysis of Fe^{2+} and In^{3+} salts does not lead to the stabilization of γ-Fe_2O_3 structure. This phase can be obtained by heating mixtures of $Fe(OH)_2$+$In(OH)_3$ or $Fe_3O_4 \cdot nH_2O$+$In(OH)_3$ sols(samples 7-10). The γ-Fe_2O_3 is the predominant phase in the samples with Fe:In = 1:1 ratio. The solubility of In^{3+} ions with the formation of solid solution is lower in spinel-type γ-Fe_2O_3 as compared to α-Fe_2O_3 phase.

Sample 5 obtained by simultaneous hydrolysis of Fe^{3+}, Fe^{2+} and In^{3+} salts is characterized by complex structure and morphology. According to the TEM and ED data, the composite consists of three phases: anisotropic particles with tetragonal structure(*Q*-γ-Fe_2O_3), spherical particles with cubic structure(*C*-γ-Fe_2O_3), and spherical particles of hexagonal α-Fe_2O_3 phase doped with In^{3+} ions. Mössbauer spectra of the composite confirm the presence of the indicated phases in 75:15:10 molar ratio[16]. IR spectra also indicate the shift of ν(Fe–O) vibration in the sample 5 comparing to the samples 7 and 9, which contain *C*-γ-Fe_2O_3 phase.

3.2 Gas-sensing properties

All studied Fe_2O_3–In_2O_3 thin-film sensors demonstrate lack of sensitivity to CH_4 and CO. This allows the fabrication of the sensors selective to other gases, in particular, to C_2H_5OH, NO_2 and O_3.

High sensitivity of several developed sensors was found to O_3 and NO_2 at low operating temperature(70-130 °C). Fig. 1 depicts the difference in the sensitivity of samples 5 and 9 having different phase composition, to the mentioned interfering gases. Thus, sample 9 is predominantly sensitive to O_3 at 100 °C. In contrast, sample 5 demon-

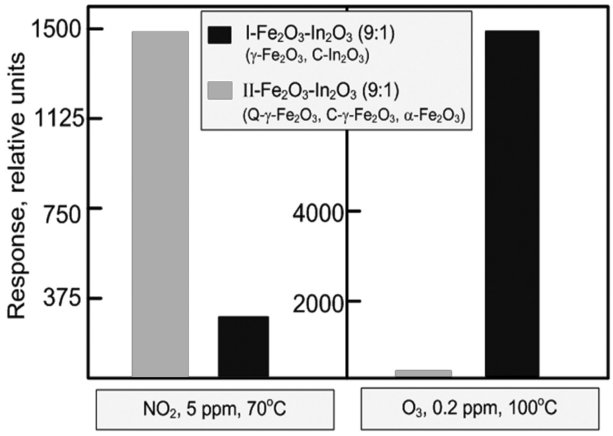

Fig. 1. Response of the Fe_2O_3–In_2O_3 sensors to NO_2 and O_3 as a function of the composite microstructure.

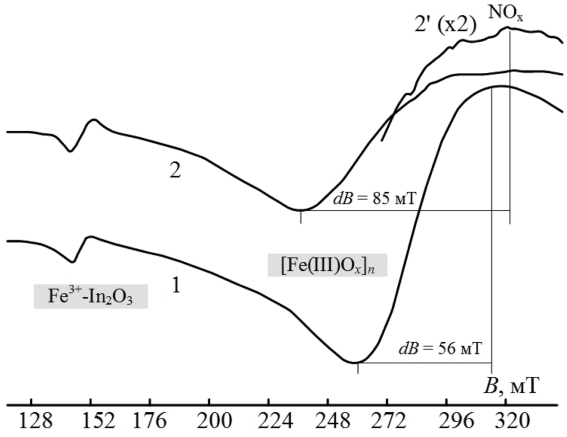

Fig. 2. EPR-spectra of sample 5, annealed at 400 °C: *1* – initial; *2* – after treatment with NO_2 at 120 °C for 30 min.

strates high response to NO_2 and no response to O_3 at 70 °C. The described phenomena can be explained by both distinctions in microstructure of the sensing layers and different mechanisms of NO_2 and O_3 detection at low-temperature region[17]. One can indicate high sensitivity to NO_2 of samples 8 and 10, consisting of *C*-In_2O_3 and *C*-γ-Fe_2O_3 phases. However, these layers are characterized by lower selectivity as compared to sample 5.

Effective detection of O_3 proceeds at film layers based on *C*-γ-Fe_2O_3 grains. Their advanced sensitivity to O_3 is caused by high adsorption ability of spinel-type γ-Fe_2O_3, fast adsorption-desorption of O_2[18], and easiness and reversibility of $Fe^{3+} + e^- \leftrightarrow Fe^{2+}$ transition[19]. *C*-γ-Fe_2O_3 phase predominates over *C*-In_2O_3 in sample 9 that causes its advanced selectivity to O_3. Note that thin film layers based on *C*-In_2O_3 also possess high sensitivity to O_3 and NO_2 at 100-150 °C[20,21]; however, they are characterized by lack of selectivity.

As a rule, high response to NO_2 is typical of the materials with small grain size and developed surface[18,22]. Adsorption mechanism of electrical conductivity change was found to be dominating for metal oxides(In_2O_3) when exposed to NO_2 at low temperatures[17,19]. Our EPR data given in Fig. 2 confirm molecular adsorption of NO_2 vapors at the surface of Fe_2O_3–In_2O_3 sample 5 at 120 °C. Exposure of the sample to NO_2 leads to the broadening of the band attributed to $(FeO)_x$ clusters and to the appearance of weak triplet signal of adsorbed NO_2 molecules(g = 2,003, A = 5.9 mT). Complex phase composition and high dispersity of sample 5 cause its high sensitivity to NO_2.

All studied Fe_2O_3–In_2O_3 composites are sensitive to C_2H_5OH vapors(50 ppm) in air at 250-350 °C. Maximum response is reached at 300 °C. However, the response varies for different samples as a function of their composition and microstructure.

As it follows from Figs. 3 and 4, the composites with equal *C*-γ-Fe_2O_3 and *C*-In_2O_3 content are the most sensitive to ethanol vapors.

The mechanism of ethanol detection by complex metaloxide layers, in particular, by Fe_2O_3–In_2O_3, is discussed in[23,24]. It is a multi-stage process including the stages of reduction-oxidation and acid-base interactions of ethanol molecules with oxide surface.

The materials containing several centers of adsorption and catalysis with close characteristics are the most sensitive to ethanol[25,26]. The occurrence of the centers of different nature in our composites provides multi-way pass of ethanol molecule decomposition and complete oxidation of intermediate products[23]. Partial reduction of metal ions without changes in phase composition is possible for some metal oxides. These oxides are effective promoters of oxidative dehydration of alcohols. In particular, easily reversible $In^{3+} \leftrightarrow In^{2+}$ and $Fe^{3+} \leftrightarrow Fe^{2+}$ equilibriums, which do not evoke phase transformations, are typical of *C*-In_2O_3 and *C*-γ-Fe_2O_3 phases. Low energy of metal-oxygen bonds in the mentioned oxides promotes oxidation of the intermediate products in the reaction of ethanol decomposition[27] that leads to the growth of sensor response.

Basing on the obtained results, Fe_2O_3–In_2O_3 materials

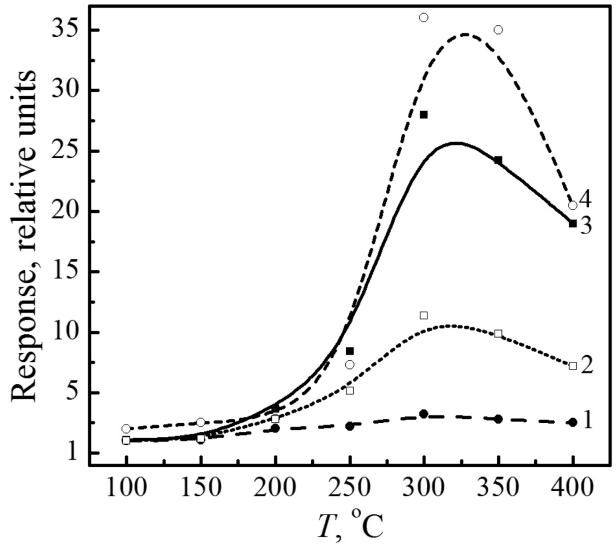

Fig. 3. Temperature-dependent response of $Fe_2O_3In_2O_3$ layers: *1* – sample 1; *2* – sample 11; *3* – sample 5; 4 – sample 7.

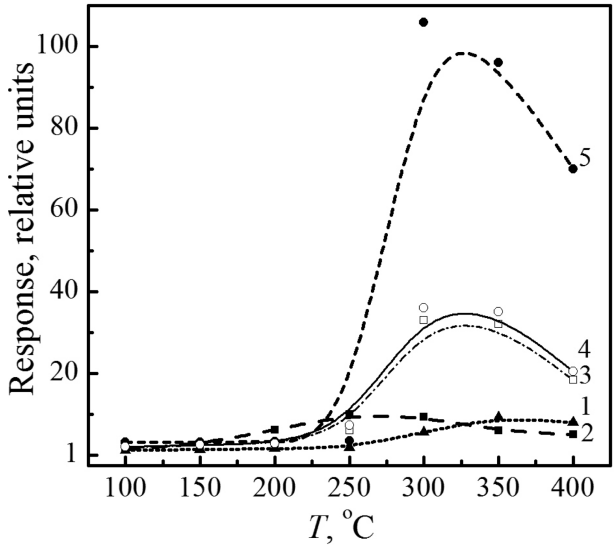

Fig. 4. Temperature-dependent response of the single oxide and $Fe_2O_3In_2O_3$ layers: *1* – In_2O_3; *2* – γ-Fe_2O_3; *3* – double-layer γ-Fe_2O_3/In_2O_3; *4* – sample 7; *5* – sample 8.

Table 2. Optimal compositions of the samples and operating conditions for selective detection of different gases

Gas	*C*, ppm	*T*, °C	*S*, r.u.	Sample No
O_3	0,1	100	130	9
NO_2	0,5	100	75	5
C_2H_5OH	50	300	120	8

suitable to produce thin-film sensors selective to O_3, NO_2 and C_2H_5OH are proposed. Optimal composition of the layers and detection conditions are given in Table 2.

4. CONCLUSIONS

Sol-gel approach based on inorganic metal precursors was used to obtain Fe_2O_3–In_2O_3 nanocomposites with different microstructure and grain size. The synthesis conditions, which result in the formation of metastable γ-Fe_2O_3 phase, were revealed. This phase stabilized in the Fe_2O_3–In_2O_3 composites was found to be more active in adsorption and catalysis as compared to thermodynamically stable α-Fe_2O_3. The Fe_2O_3–In_2O_3 compositions suitable for the selective detection of O_3, NO_2 and C_2H_5OH were proposed.

ACKNOWLEDGMENT

The authors thank Korean Sensors Society and the International Science and Technology Center(ISTC) for financial support and organization of 27th Korea-ISTC workshop.

REFERENCES

[1] M. Ivanovskaya, P. Bogdanov, D. Orlik, and A. Gurlo, "Gas-sensitive properties of metaloxide sensors prepared by sol-gel technique", *Proc. VI NEXUSPAN Workshop*, pp. 2529-2532, Kaunas, Lithuania, 1999.

[2] M. Ivanovskaya, P. Bogdanov, and A. Gurlo, "Sol-gel obtained oxide composites: structure and gas-sensitivity", *Proc. VIII Int. Meet. Chem. Sensors*, p. 94, Basel, Switzerland, 2000.

[3] C.J. Brinker and G.W. Scherer, *Sol-gel science*, 502, AP, London, 1990.

[4] E.V. Frolova and M.I. Ivanovskaya, "Structural defects formation in the inorganic sol-gel derived oxides", *Defect and Diffusion Forum*, vol. 242-244, pp. 143-258, 2005.

[5] U. Schwertmann and R.M. Cornell, *Iron oxides in the laboratory*, VCH Verlagsgesellschaft mbH, Weinhem, 138, 1991.

[6] J.L. Jambor and J.E. Dutrizac, "Occurrence and constitution of natural and synthetic ferrihydrite, a widespread iron oxyhydroxide", *Chem. Rev.*, vol. 98, pp. 2549-2585, 1998.

[7] L. Smart and E. Moore, *Solid state chemistry*, 379, Chapman & Hall, London, 1995.

[8] A. Gurlo, M. Ivanovskaya, N. Barsan, and U. Weimar, "Corundum-type indium(III) oxide: formation under ambient conditions in Fe_2O_3-In_2O_3 system", *Inorg. Chem. Comm.*, vol. 6, pp. 569-572, 2003.

[9] D. Kotsikau, M. Ivanovskaya, D. Orlik, and M. Falasconi, "Gas-sensitive properties of thin- and thick-film sensors based on Fe_2O_3-SnO_2 nanocomposites", *Sens. Actuators B*, vol. 101, pp. 199-206, 2004.

[10] D. Orlik, M. Ivanovskaya, and A. Gurlo, "Properties of ceramic semiconductor sensors based on SnO_2–Sb_2O_3", *Russ. J. Anal. Chem.*, vol. 52, no. 1, pp. 69, 1997.

[11] M. Ivanovskaya, "Ceramic and film metaloxide sensors obtained by sol-gel method: structural features and gas-sensitive properties", *Electron Technol.*, vol. 33, pp. 108-112, 2000.
[12] V. Golovanov, C-C. Liu, A. Kiv, D. Fuks, and M. Ivanovskaya, "Microfabricated one-electrode In_2O_3 and Fe_2O_3–In_2O_3 composite sensors", *Comp. Model. New Technol.*, vol. 13, no. 2, pp. 70-75, 2009.
[13] M. Ivanovskaya, D. Kotsikau, G. Faglia, P. Nelli, and S. Irkaev, "Gas-sensitive properties of thin film heterostructures based on Fe_2O_3-In_2O_3 nanocomposites", *Sens. Actuators B*, vol. 93, pp. 422-430, 2003.
[14] G. Ennas, G. Marongui, A. Musinu, A. Falqui, P. Ballirano, and R. Caminity, "Characterization of nanocrystalline γ-Fe_2O_3 prepared by wet chemical method", *J. Mater. Res.*, vol. 14, no. 4, pp. 1570-1575, 1999.
[15] M. Macias, J. Morales, J.C. Tirado, and C. Valera, "Effect of crystallinity on the thermal evolution of γ-Fe_2O_3", *Thermochim. Acta*, vol. 133, pp. 107-112, 1998.
[16] M. Ivanovskaya, D. Kotsikau, A. Taurino, and P. Siciliano, "Structural distinctions of Fe_2O_3-In_2O_3 composites obtained by various sol-gel procedures, and their gas-sensing features", *Sens. Actuators B*, vol. 124, pp. 133-142, 2007.
[17] M. Ivanovskaya, A. Gurlo, and P. Bogdanov, "Mechanism of O_3 and NO_2 detection and selectivity of In_2O_3 sensors", *Sens. Actuators B*, vol. 70, no. 1-2, pp. 264-267, 2001.
[18] V.V. Lunin, M.P. Popovich, and S.N. Tkachenko, *The physical chemistry of ozone*, pp. 480, Moscow State University, Moscow, 1998.
[19] E. Gutman, "Ozone sensor for the earth ozonosphere investigations", *Sens. Actuators B*, vol. 25, pp. 135-146, 1996.
[20] A. Gurlo, N. Barsan, M. Ivanovskaya, U. Weimar, and W. Göpel, "In_2O_3 and In_2O_3-MoO_3 thin film semiconductor sensors: interaction with NO_2 and O_3", *Sens. Actuators B*, vol. 47, pp. 92-99, 1998.
[21] M. Ivanovskaya, P. Bogdanov, G. Faglia, and G. Sberveglieri, "The features of thin film and ceramic sensors for the detection of CO and NO_2", *Sens. Actuators B*, vol. 68, pp. 344-350, 2000.
[22] V.Ya. Sukharev, and I.A. Myasnikov, "Theoretical base of semiconducting sensors in analysis of active gases. Influence of adsorption of gases on electrical conductivity of polycrystalline sorbents", *Russ. J. Phys. Chem.*, vol. 61, no. 2, pp. 302-312, 1987.
[23] M. Ivanovskaya, P. Bogdanov, G. Faglia, P. Nelli, and G. Sberveglieri, "On the role of catalytic additives in gas-sensitivity of SnO_2-based thin film sensors", *Sens. Actuators B*, vol. 70, no. 1-2, pp. 268-274, 2001.
[24] M. Ivanovskaya, D. Kotsikau, G. Faglia, and P. Nelli, "Influence of chemical composition and structural factors of Fe_2O_3/In_2O_3 sensors on their selectivity and sensitivity to ethanol", *Sens. Actuators B*, vol. 96, pp. 498-503, 2003.
[25] G.I. Golodets, *Reductive-oxidative and acid-base steps of heterogeneous catalytic oxidising reaction, Catalysis mechanism,* part. 1, pp. 142-158, Nauka, Novosibirsk, 1984.
[26] O.V. Krylov, *The catalysis by non-metals. The appropriateness of the catalysts selection*, pp. 240, Khimia, Leningrad, 1967.
[27] D. Kohl, "Surface processes in the detection of reducing gases with SnO_2-based devices", *Sens. Actuators B*, vol. 18, pp. 71-113, 1989.